

Fabrication of an Optical Silicon Accelerometer with Antiresonant Waveguides

A. Llobera¹, J. A. Plaza¹, I. Salinas², J. Berganzo³, J. Garcia³, J. Esteve¹ and C. Domínguez¹
 1. IMB-CSIC. Campus UAB 08193 Cerdanyola, Barcelona, Spain. andreu.llobera@cnm.es
 2. Dept. de Física Aplicada, Universidad de Zaragoza
 3. Ikerlan, Departamento de Electrónica y Componentes

SUMMARY

The fabrication and characterization of an optical accelerometer based on Silicon technology and using BESOI wafers is presented. Instead of the standard total internal reflection (TIR) waveguides, ARROW (AntiResonant Reflecting Optical Waveguides) have been used. On the basis of a quad beam accelerometer design, a sensing waveguide has been placed on the seismic mass. Its misalignment with the waveguides located at the frame allows measuring acceleration changes. The mechanical structure has been designed so as to have a span of $2\mu\text{m}$, that should provide with a sensitivity of 4dB/g. Reference waveguides measured by end-fire coupling have low radiation and insertion losses (0.3 dB/cm and 2.5 dB, respectively). However, when V-grooves with glass anodic bonding are used, high insertion losses are observed, due to imperfections in polishing. This fact causes the reduction of its sensibility to 2.5dB/g

Keywords: Opto-mechanical sensors, MOEMS, Integrated optics, Technology

Subject category: 5. Physical sensors (non-magnetic)

INTRODUCTION

To overcome the inherent problems of electrical-based accelerometers, as could be temperature dependence, low sensitivity and non stable output under electromagnetic interference (EMI) [1], there has been several proposals of optical-based accelerometers, both using integrated optics [2] and fiber optics [3]. The complete immunity against EMI and the possibility of having the light sources far from the device also makes them extremely useful in highly explosive atmospheres or where a strong electromagnetic field is present.

Up to date, the most common light guiding structures used on optical accelerometers have a high refractive index etched layer (frequently silicon nitride) in a cantilever configuration. Although they could be considered as optimum for MOEMS applications, it has to be noted that these waveguides normally have thicknesses around $0.2\mu\text{m}$. If it is taken into account that a standard monomode optical fiber has a $4\mu\text{m}$ core, the high difference between the cross section of both structures is the main responsible of the high insertion losses (>20dB) of

these waveguides in the visible range when light is inserted by end-fire coupling.

ARROW structures have received recently much attention due to its interesting properties [4]. Guiding in these waveguides is achieved via the Fabry Perot interferometer placed beneath the core, as seen in fig. 1. There exist some values for d_1 and d_2 where a maximum reflection at the core-1st cladding boundary is observed (>99.96%) for the TE₀. At the upper core-air boundary, the guiding is caused by standard TIR. Higher order modes are filtered out since the antiresonant layers are not properly sintonized. Hence, this structure has monomode behavior for core thickness of the same size as the fiber optics, minimizing the insertion losses.

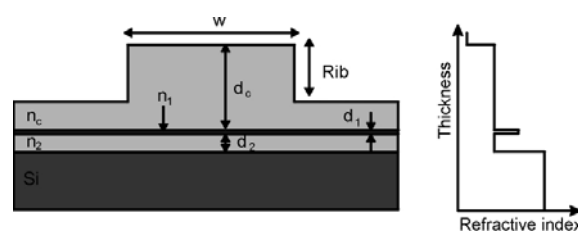


Fig. 1: Standard configuration and refractive index profile of ARROW structures. The darker the grey, the higher the refractive index is.

DESIGN & SIMULATION

Firstly, an optical analysis of the accelerometer, as depicted in fig 2, was simulated. Although $\text{Si}_3\text{N}_4/\text{SiO}_2$ -based ARROW structures had previously been studied [5], it was necessary to analyze the effects of the misalignment between the waveguide on the seismic mass and the waveguides located at the frame. To avoid the excessive losses caused by the beam broadening, waveguides were increasingly wider at each cut.

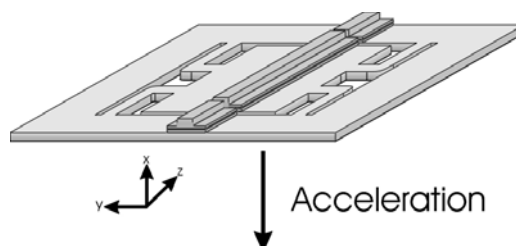


Fig. 2: Scheme of the quad beam optical accelerometer design.

Optical simulations of the total device losses as a function of the seismic mass displacement were done by Finite Difference Method (FDM) together with the Beam Propagation Method (BPM). Fig. 3 shows a lateral view of the light intensity propagating through the device. When all waveguides are aligned (3a), a minimum loss is presented. As the seismic mass starts moving, the misalignment causes a sharp increase of the losses (3b & 3c). If the seismic mass is broken, that is, if there is no intermediate waveguide, losses reach its maximum, as observed in fig. 3d. Hence, it was possible to define a highly-sensitive linear region ($>4\text{dB/g}$) into which the optical accelerometer should be sintonized so as to have optimal properties.

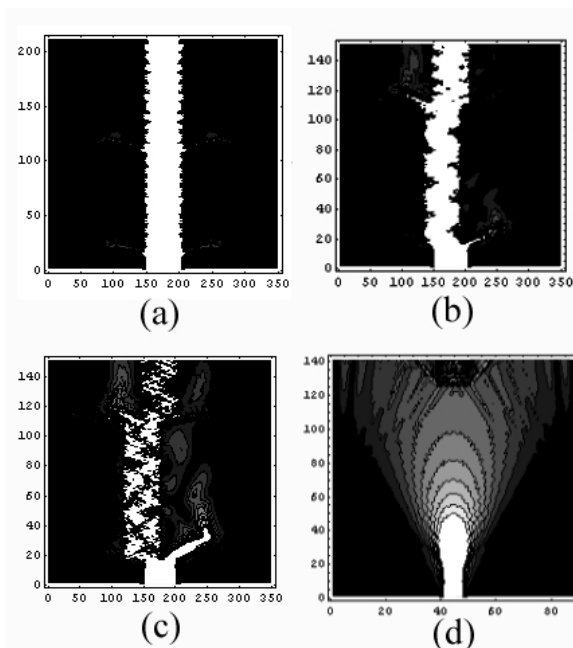


Fig. 3: Optical simulation of the waveguide misalignment: a) no misalignment. b) 30% misalignment. c) 60% misalignment. d) without intermediate waveguide

Once the working region was established, the mechanical properties were chosen so as to fulfill the optical requirements. Mechanical optimization of the structure was done via the Finite Element Method (FEM) using ANSYS 5.7. Accelerometer quad-beam configuration was chosen since it provides with flat vertical movement when acceleration is applied orthogonal to the device, as shown in fig. X. It was designed to have a $1\mu\text{m/g}$ of mechanical sensitivity. The cross-sensitivities were also simulated and are presented in table 1. It can be observed that although misalignment obtained matched with the expected mass movement, there exists a significant crossed acceleration effects: The misalignment between the waveguides on the frame and on the mass is $0.202\mu\text{m/g}$ for x-accelerations and 0.105 for y-accelerations. It has to be noted, however, that since

the waveguide is located at the center of the seismic mass, movements on the y direction would not affect its relative position. Thus, the device is completely insensitive to accelerations in the y direction. Modal simulations were done to estimate the natural frequency of the devices. The simulated frequency for the first modal mode is 489 Hz.

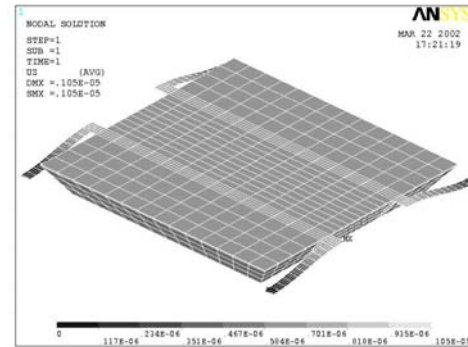


Fig 4: Deformation of the accelerometer when submitted to 1g acceleration in the z axis

Table 1: Maximum displacement of the mass and misalignment between the waveguides on the frame and on the mass versus the three directions of the acceleration.

Acceleration [g]	Maximum mass displacement	Waveguides misalignment
Z-direction	$1.050\mu\text{m}$	$1.050\mu\text{m}$
Y-direction	$0.105\mu\text{m}$	$0.105\mu\text{m}$
X-direction	$0.202\mu\text{m}$	$0.202\mu\text{m}$

FABRICATION

Accelerometers were fabricated on a N type, (100) oriented, $450\mu\text{m}$ thick BESOI (Bond and Etch Back Silicon On Insulator) wafers from ShinEtsu. Thickness of the upper silicon and buried silicon layers are $15\mu\text{m}$ and $2\mu\text{m}$, respectively. In these substrates is grown the second cladding layer ($2\mu\text{m}$ of silicon dioxide), obtained by wet oxidation at 1000°C . First cladding is a $0.38\mu\text{m}$ LPCVD silicon nitride for ARROW-A obtained at 700°C . Core layer consists in a PECVD-deposited silicon oxide, with refractive index $n=1.485$. This layer is $3.5\mu\text{m}$ etched using RIE in order to assure cross section confinement. Finally, a $2\mu\text{m}$ PECVD silicon oxide layer was deposited over the waveguides so as to protect them against dust or scratches that would cause an increase of the device losses, not due to the working principle, but to defects in its guiding structures.

The following step was the complete removal of all the ARROW layers but in the zone where the rib has been defined (fig. 5). Concretely, the technological process mask has been designed so as to leave the ARROW structure only at $100\mu\text{m}$ in distance from the rib. This is has been done so

because of the fact that it is expected that the accelerometer does not suffer from the so-called bimetal effect, that is, bending of the structures due to the different expansion coefficient of two or more layers one above the other. Thus, it is essential to remove all silicon oxide and silicon nitride in the region where the mechanical structure has to be defined.

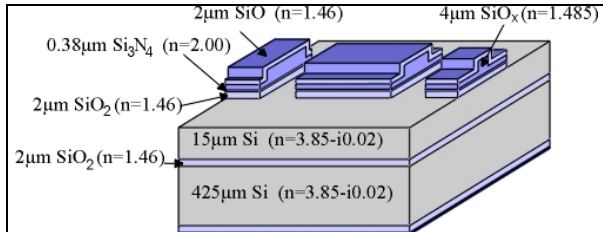


Fig 5: Wafer status after ARROW waveguide definition and removal of all layers where unnecessary.

Layer thicknesses to be etched are significantly high. This forces using aluminium as a mask.. Micromechanical structure has been defined in two steps: Firstly, an anisotropic etch in KOH at the back side of the wafer has provided with the three-dimensional structure. Anisotropic etching is done in KOH. As compared to TMAH, the former has a higher selectivity on etching (100) and (111) planes (which provides with a better accuracy on obtaining the expected geometry) and a minor lateral etching (which allows defining smaller convex corner compensation structures). Moreover, due to the KOH selectivity, either in the (111) and silicon oxide etching speed, the etching is automatically stopped at (111) planes and when the buried silicon oxide layer is reached (fig. 6). Once the accelerometer has been defined at the back side, a RIE etching by the front side has liberated the seismic mass from the buried silicon oxide.

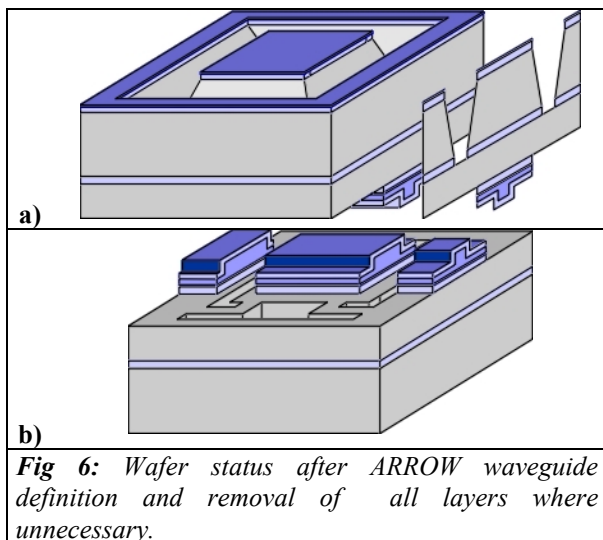


Fig 6: Wafer status after ARROW waveguide definition and removal of all layers where unnecessary.

Although the accelerometer fabrication could be considered as finished at this point, the devices are extremely fragile and easily crack. For this reason a wafer glass (Pyrex #7740) previously mechanized was bonded on the back side of the silicon wafer, as shown in fig. 7.

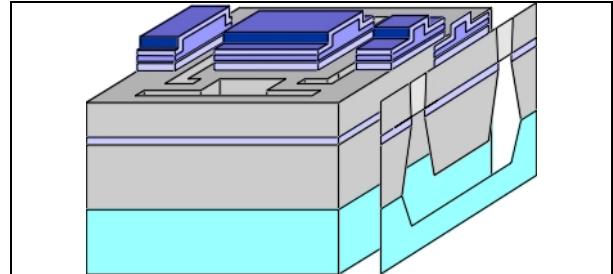


Fig 7: Wafer status at the end of the fabrication process, when a Pyrex wafer has been anodically bonded to the back of the accelerometer

Once the accelerometers were obtained, problem arise from the fact that it was necessary to align the device with the fiber optics, placed in the V-groove. In order to achieve appropriate light transmission, The accelerometer is firstly fixed to a mechanized aluminium piece that has a slight minor length than the accelerometers. V-Grooves are then able to move in the three axis until they are correctly aligned, being then stacked. When the glue is dried, two self-aligned pieces are placed underneath the V-grooves so as to provide the whole structure with robustness. The final appearance of the device is shown in fig. 8

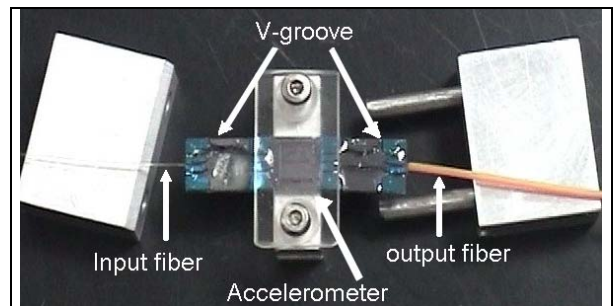


Fig 8: Pre-packaging of the accelerometer and V-grooves with fiber optics on aluminium mechanized structure

CHARACTERIZATION

Reference waveguides were measured by end-fire coupling so as to determine the radiation and insertion losses at $\lambda=633\text{nm}$ provided with a results of 0.3dB/cm and 2.5dB respectively. However, First experimental results showed that the device had losses of 29dB. When V-grooves were aligned to the accelerometer, losses even had a more dramatic value, since they increased until 35.1dB. However, after stacking both structures with the appropriate glue, they were lowered to 18.3dB. This factor is a

factor 2 higher as compared to the values obtained by simulations. This fact could be associated to errors during the V-grooves polishing. Nevertheless, power obtained at the output allows appropriate optical characterization.

Accelerometer response as a function of the gravitational field was measured using a Ferris wheel that has a controlled angular movement in such a way that the acceleration applied to the device is the projection of this magnitude to the sensible axis of the device. Results can be seen in fig. 9. As can be observed the expected periodical response as a function of the angle is obtained. It has to be noted that losses shown in this figure have been re-ranged, being the zero fixed for the maximum power output. This is has been done so as to determine the optical accelerometer sensitivity. It can be observed that minimum losses are not obtained at 90° and 270°, which provide with an acceleration of 0g, but have a slight displacement to 100° and 270°. This value corresponds to a misalignment between waveguides of 0.18µm.

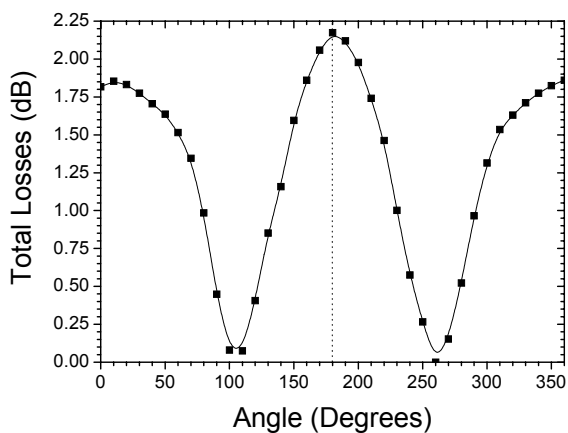


Fig. 9: Accelerometer output intensity as function of the gravity field tilt.

Although the behaviour between the two minimum losses presents a very high linearity, it can be observed that seismic mass displacement does not cause symmetrical power variations, since at the region between 0 and 90° (and also between 270° and 360°) a tail is observed in the experimental data. This fact could be understood if it is taken into account that waveguides have passivation. When the accelerometer suffers from large negative values of the acceleration, light is partially injected to the passivation, causing a decrease of the losses. This fact is not observed at positive acceleration values since the light injected in the 2nd cladding is fastly absorbed by the silicon of the seismic mass.

CONCLUSIONS

An optical accelerometer based on antiresonant waveguides has been designed so as to have an

optical sensitivity of 4dB/g. The fabrication process using BESOI wafers has proved its viability and reference waveguides presented the expected low radiation and insertion losses (0.3dB/cm and 2.5dB) at the working wavelength. Although inappropriate polishing of the V-grooves have caused a significant increase of the insertion losses, measurements done have provided with the expected periodical response of the losses as a function of the gravitational field. Measurements done have proved that waveguides only are 0.18µm misaligned, with a highly lineal but asymmetric response, due to the passivation.

ACKNOWLEDGMENTS

A. Llobera thanks the Generalitat de Catalunya (Catalan Council) for grant 2001-TDOC-00008.

REFERENCES

- [1] N.Yazdi, F.Ayazi, K.Najafi. *Micromachined Inertial Sensors*. *Proced. IEEE* 86[8], 1640-1659. 1998.
- [2] J.M.López-Higuera, P.Mottier, et al. *Optical Fiber and Integrated Optics Accelerometers for Real Time Vibration Monitoring in Harsh Environments: In-Lab and in-Field Characterization*. *Europ.Works.Opt.Fib. Sens.(SPIE)* 3483, 223-226. 1998.
- [3] J.Kalenik, R.Pajak. *A Cantilever Optical-fiber Accelerometer*. *Sens.& Act.A* 68, 350-355. 1998.
- [4] T.Baba, Y.Kokubun. *Dispersion and Radiation Loss Characteristics of Antiresonant Reflecting Optical Waveguides-Numerical Results and Analytical Expressions*. *J.Quant.Elect.* 28[7], 1689-1700. 1992.
- [5] I.Garcés, F.Villuendas, et al. *Analysis of Leakage Properties and Guiding Conditions of Rib Antiresonant Reflecting Optical Waveguides*. *J.Light.Tech.* 14[5], 798-805. 1996.